Geochemistry, Geophysics, Geosystems

RESEARCH ARTICLE
10.1029/2020GC008941

Soil and Air Temperature Calibrations Using Branched GDGTs for the Tropical Andes of Colombia: Toward a Pan-tropical Calibration

Lina C. Pérez-Angel[1,2,3], Julio Sepúlveda[1,3], Peter Molnar[1,2], Camilo Montes[4], Balaji Rajagopalan[2,5], Kathryn Snell[1], Catalina Gonzalez-Arango[6], and Nadia Dildar[1,3]

[1]Department of Geological Sciences, University of Colorado Boulder, Boulder, CO, USA, [2]Cooperative Institute for Research in Environmental Sciences, University of Colorado Boulder, Boulder, CO, USA, [3]Institute of Arctic and Alpine Research (INSTAAR), University of Colorado Boulder, Boulder, Colorado, USA, [4]Department of Physics and Geosciences, Universidad del Norte, Barranquilla, Colombia, [5]Department of Civil, Environmental and Architectural Engineering, University of Colorado Boulder, Boulder, CO, USA, [6]Department of Biological Sciences, Universidad de Los Andes, Bogotá, Colombia

Key Points:
- New regional soil and air brGDGT linear calibrations for the Eastern Cordillera of Colombia have RMSEs of 1.5°C and 1.9°C, respectively
- A soil linear calibration for the tropics has a RMSE of 2.7°C, compared with global calibrations with RMSEs of 3.8–4.9°C
- A nonlinear calibration for the tropics yields a RMSE of 2.2°C

Supporting Information:
- Figure S1
- Table S1
- Table S2
- Table S3
- Table S4

Correspondence to:
L. C. Pérez-Angel,
lina.perezangel@colorado.edu

Citation:
Pérez-Angel, L. C., Sepúlveda, J., Molnar, P., Montes, C., Rajagopalan, B., Snell, K., et al. (2020). Soil and air temperature calibrations using branched GDGTs for the Tropical Andes of Colombia: Toward a pan-tropical calibration. *Geochemistry, Geophysics, Geosystems*, *21*, e2020GC008941. https://doi.org/10.1029/2020GC008941

Received 22 JAN 2020
Accepted 6 JUL 2020
Accepted article online 14 JUL 2020

Abstract Branched glycerol dialkyl glycerol tetraethers (brGDGTs) are bacterial cell membrane lipids that, when preserved in sedimentary archives, can be used to infer continental paleotemperatures. Although commonly used global calibrations capture a relationship between the distribution of brGDGTs and temperature, they underestimate temperatures for tropical regions as much as ~16°C. Furthermore, some global calibrations reach saturation at around 24–25°C, and, in general, they have root-mean-squared errors (RMSEs ≈ ~4°C) that are too large for them to resolve small variations in paleoclimate variability in tropical regions. We present an *in situ* regional calibration of soil brGDGTs along altitudinal transects on both flanks of the Eastern Cordillera of Colombia in the northern tropical Andes that spans ~3,200 m in elevation and 17°C and 19°C in mean annual soil and air temperatures, respectively. These new soil and air regional calibrations yield RMSEs of 1.5°C and 1.9°C, respectively. When combined with existing data from elsewhere in the tropics, the integrated data ($n = 175$) not only fit a linear calibration with a RMSE of 2.7°C but also fit a nonlinear calibration with a RMSE of 2.2°C. These calibrations allow for a more precise and reliable reconstruction of past temperatures in the tropics than global calibrations.

Plain Language Summary Small variations in temperatures within the tropics can have large effects on climate at middle and high latitudes. A common example is how the El Niño Southern Oscillation (ENSO) can alter climate around the world. Quantitative terrestrial temperature records from the tropics, however, are scarce. A paleotemperature proxy, based on the abundances of different bacterial cell membrane lipids, has enabled quantitative estimates of continental temperature, but the uncertainties in these global estimates remain large (3.8–4.9°C). Because past temperature changes in the tropics are small relative to other regions, high-precision temperature estimates are necessary to evaluate small changes that could have bigger effects elsewhere. We generated new data from the Eastern Cordillera of Colombia to estimate air and soil temperatures using this lipid-based proxy. In order to improve temperature reconstructions within the tropics, we compiled tropical soil data within 23.5° of the equator to provide a calibration for this latitudinal range.

1. Introduction

Small variations in temperatures within the tropics can have large effects on climate at higher latitudes, as illustrated by teleconnections from the Eastern Tropical Pacific and the El Niño Southern Oscillation (ENSO) (e.g., Halpert & Ropelewski, 1992; Ropelewski & Halpert, 1987, 1989; Sarachik & Cane, 2010; Trenberth et al., 1998). It follows that past mid-latitude climates may also reflect, and perhaps result from, variations in tropical conditions. Most quantitative estimates of past temperature from the tropics, however, come from marine sediment (e.g., Dekens et al., 2007; Groeneveld et al., 2006; Herbert et al., 2016, 2010; Lawrence et al., 2006; Ravelo et al., 2006; Wara et al., 2005; Zachos et al., 2001). Paleoclimate reconstructions from continental regions in the tropics are scarce (e.g., Anderson et al., 2015; Loomis et al., 2015; Salzmann et al., 2013) and, in many cases, qualitative (e.g., Hooghiemstra et al., 2006; Torres et al., 2005; van der

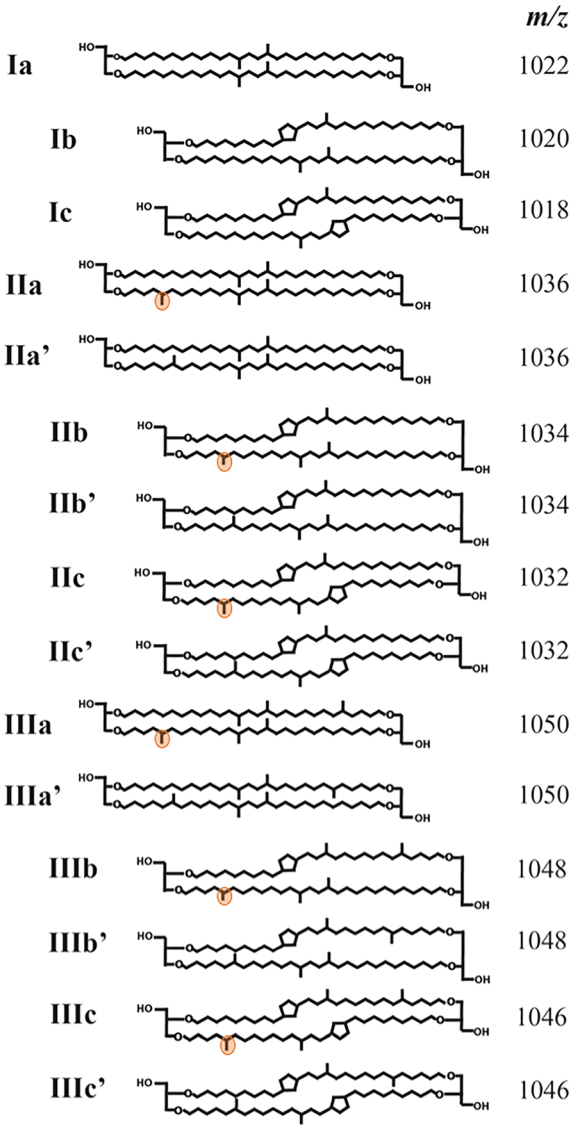

Figure 1. Chemical structures of brGDGTs used in this study. Each letter corresponds to different structure from a methyl to a cyclopentyl moiety: 'a' structures have no cyclopentyl moieties, 'b' structures have one cyclopentyl moiety, and 'c' structures have two cyclopentyl moieties. The structures with C6-methylation are referenced with a prime symbol. C5-methylations are highlighted in orange in the corresponding structure. Figure is modified from Hanna et al. (2016).

Hammen et al., 1973). Missing has been a well-calibrated proxy that quantifies past terrestrial temperatures and that can be applied widely to past tropical environments.

Bacterial branched glycerol dialkyl glycerol tetraethers (brGDGTs) have evolved as a tool for the quantitative reconstruction of past continental temperatures (e.g., De Jonge et al., 2014; Lu et al., 2016; Peterse et al., 2014, 2012; Thomas et al., 2017; Weijers et al., 2007; Yamamoto et al., 2016). The development of these proxies has been particularly relevant in places where sedimentary rocks with organic matter may not preserve other materials useful for temperature reconstructions, such as carbonates and fossil leaves (e.g., Ghosh et al., 2006; Wolfe, 1995). To enable accurate estimates of past temperatures in tropical environments, we calibrated brGDGTs in soils as a paleotemperature proxy. We measured both air and soil temperatures and brGDGTs along two altitudinal transects across the Eastern Cordillera of Colombia to construct regional calibrations for each. We then incorporated published data from soils elsewhere in the tropics (De Jonge et al., 2014; Dearing Crampton-Flood et al., 2020; Jaeschke et al., 2018; Naafs, Gallego-Sala, et al., 2017; Wang et al., 2020) to derive a pantropical calibration of air temperatures.

2. Background on brGDGTs

brGDGTs are cell membrane lipids (Figure 1) produced by bacteria in soils, peats, lakes, marine sediment, and anoxic water columns (Liu et al., 2010, 2012, 2014; Russell et al., 2018; Sinninghe Damsté et al., 2000; Weber et al., 2015, 2018; Weijers et al., 2006, 2007). Early studies demonstrated that the distribution of brGDGTs in soils, expressed as the cyclization of branched tetraethers (CBTs) and the methyl index of branched tetraethers (MBTs), correlated with the pH of the soil and mean annual air temperature (MAAT), respectively (Weijers et al., 2007). Peterse et al. (2012) refined this MBT index by excluding brGDGTs IIIb and IIIc, because, in general, they are found in low abundance and below the analytical limit of detection. When incorporated in globally distributed soil data sets and calibrations, this new index (MBT′) allows for the reconstruction of past MAAT (Peterse et al., 2012).

More recently, using an improved chromatographic method capable of separating 5- and 6-methyl isomers, De Jonge et al. (2014) demonstrated that although 5-methyl brGDGTs were mostly influenced by temperature, 6-methyl brGDGTs correlate with pH. By including only 5-methyl brGDGTs from globally distributed soil samples, De Jonge et al. (2014) produced a new methylation index (MBT'_{5me}):

$$MBT'_{5me} = \frac{(Ia + Ib + Ic)}{(Ia + Ib + Ic + IIa + IIb + IIc + IIIa)}. \quad (1)$$

Then, they used the MBT'_{5me} index to produce a simple linear equation that relates it to MAAT, independently of soil pH:

$$MAAT = -8.57 + 31.45 \times MBT'_{5me} \left(n = 231, R^2 = 0.64, \mathrm{RMSE} = 4.9°\mathrm{C}\right), \quad (2)$$

where n is the number of samples used in the calibration, R^2 is the coefficient of determination between MAAT and the combination of individual brGDGTs, and RMSE is the root-mean-squared error of

temperature in the respective calibration. Each term in the equation, and illustrated in Figure 1, uses the fractional abundance (FA) of each individual compound, which is calculated as the relative abundance of a particular brGDGT to the total abundance of brGDGTs in a sample.

The MBT'_{5me} index, as all previous MBT indices based on ratios, is a fraction whose maximum possible value is one. When the MBT'_{5me} index reaches one ($MBT'_{5me} = 1$), 2 allows for the reconstruction of MAAT only up to 22.7°C, and therefore, this equation does not allow a reliable reconstruction of MAAT in tropical regions, where temperatures commonly exceed 22.7°C. To expand the range of temperature that can be reconstructed, De Jonge et al. (2014) proposed a multiple linear regression using the FA of individual 5-methyl brGDGTs (Figure 1):

$$\mathrm{MAAT_{mr}} = 7.17 + 17.1 \times [\mathrm{Ia}] + 25.9 \times [\mathrm{Ib}] + 34.4 \times [\mathrm{Ic}] - 28.6 \times [\mathrm{IIa}] \quad (3)$$

$$\left(n = 222, R^2 = 0.68, \mathrm{RMSE} = 4.6°\mathrm{C}\right).$$

Their inferences of temperature with samples used in the calibration, however, extend only to ~26°C, and extrapolating to higher temperatures must be done with caution.

More recently, Naafs, Gallego-Sala, et al. (2017) refined these global calibrations by filtering samples from the globally distributed soil compilation using the relative abundance of 6-methyl brGDGTs (IR_{6me} index) proposed by Dang et al. (2016):

$$\mathrm{IR_{6me}} = \frac{[\mathrm{IIa'}] + [\mathrm{IIb'}] + [\mathrm{IIc'}] + [\mathrm{IIIa'}] + [\mathrm{IIIb'}] + [\mathrm{IIIc'}]}{[\mathrm{IIa'}] + [\mathrm{IIb'}] + [\mathrm{IIc'}] + [\mathrm{IIIa'}] + [\mathrm{IIIb'}] + [\mathrm{IIIc'}] + [\mathrm{IIa}] + [\mathrm{IIb}] + [\mathrm{IIc}] + [\mathrm{IIIa}] + [\mathrm{IIIb}] + [\mathrm{IIIc}]}. \quad (4)$$

Dang et al. (2016) found that correlation between MBT'_{5me} and MAAT was higher in soils with ratios of 6- over 5-methyl brGDGTs lower than 0.5 ($IR_{6me} < 0.5$) than in those with $IR_{6me} > 0.5$. After excluding 173 soils from the globally distributed soil compilation of De Jonge et al. (2014) with $IR_{6me} > 0.5$, Naafs, Gallego-Sala, et al. (2017) proposed two new air temperature calibrations with higher R^2 and lower RMSEs than those of De Jonge et al. (2014):

$$\mathrm{MAAT_{soil5me}} = -14.5 + 39.09 \times \mathrm{MBT'_{5me}} \left(n = 177, R^2 = 0.76, \mathrm{RMSE} = 4.1°\mathrm{C}\right), \quad (5)$$

and

$$\mathrm{MAAT_{mrlsoil5me}} = 10.0 + 14.7 \times [\mathrm{Ia}] - 31.7 \times [\mathrm{IIa}] \left(n{=}177, R^2{=}0.77, \mathrm{RMSE}{=}3.8°\mathrm{C}\right). \quad (6)$$

These two calibrations, however, cannot be used to estimate temperatures above 24–25°C; when the $MBT'_{5me} = 1$ in 5, the estimated temperature saturates at 24.6°C. For 6, the maximum temperature that this calibration can estimate is 24.7°C, when the FA of brGDGT Ia = 1 and brGDGT IIa = 0. Dearing Crampton-Flood et al. (2020) used a Bayesian calibration method for globally distributed soils and peats that enabled an upper limit of their calibration of ~28°C.

Despite these efforts to improve the global calibration of brGDGT proxies, the scatter in derived temperature estimates remains large, RMSEs ≈ 3.8–4.9°C, while the range of residuals can be larger than ~15°C. Moreover, environmental factors besides temperature may affect the production of brGDGTs through their source organisms and their distribution in the environment. Precipitation, soil moisture, vegetation cover, differences in bacterial community composition, and growing degree days (GDDs) of the source organism above freezing are all known sources of variability in the distribution of brGDGTs in soils (Dang et al., 2016; De Jonge et al., 2019; Liang et al., 2019; Menges et al., 2014; Naafs, Gallego-Sala, et al., 2017; Peterse et al., 2014; Wang et al., 2014). These environmental factors can vary regionally and thus affect the sources and distribution of brGDGTs (Ding et al., 2015; Menges et al., 2014; Wang et al., 2016; Yang et al., 2015). Furthermore, the biological source of brGDGTs remains unknown, but they are ubiquitous in nature and are found in a wide range of environments. Acidobacteria were suggested to represent the most likely source of brGDGTs in a soil profile from the Saxnås Mosse peat bog (Weijers et al., 2009). So far, only a small number of acidobacteria grown in culturing studies have been shown to produce brGDGTs, and only a limited

number of such brGDGTs (Sinninghe Damsté et al., 2018, 2011). Recently, De Jonge et al. (2019) reported a difference in bacterial community composition in two clusters of Icelandic soils with temperatures <14°C and >14°C. Since the variability in brGDGTs between these cold and warm clusters cannot be solely explained by membrane adaptation to temperature on the same bacterial community, the result implied a difference in the brGDGTs producers. Furthermore, Weber et al. (2018) showed a redox-dependent differentiation in the bacterial community in a stratified lake system with strong redox gradients, which impacts the distribution of brGDGTs at different water depths. The biological sources of brGDGTs not only remain largely unknown, but these lipids have also been found in a wide range of environments. Therefore, given the large diversity of bacteria in soils, the few taxa that account for almost half of this diversity, and the role of environmental factors controlling their distribution (Delgado-Baquerizo et al., 2018), it is reasonable to assume that multiple biological sources of brGDGTs are possible in different types of soils, as De Jonge et al. (2019) recognized.

Soil bacteria sense the temperature in the soil not that of the overlying air. Therefore, scatter in inferences of MAATs may also derive from temperature differences between the soil and air. Finally, uncertainty of whether bacteria grow in some, but not all, seasons and in how they sense seasonal variations in temperature adds uncertainty to inferences of temperatures, especially in globally distributed soil samples spanning different latitudes with differing amplitudes of annual temperature variation (Dearing Crampton-Flood et al., 2020; Deng et al., 2016; Naafs, Inglis, et al., 2017; Wang et al., 2016; Yang et al., 2014). The modest seasonal cycle in the tropics makes temperature differences between MAAT and, for example, the warmest month, generally smaller than uncertainties in temperature estimates based on these calibrations.

3. Material and Methods

3.1. Sampling in the Eastern Cordillera of Colombia

We collected 32 soil samples from 5 to 10 and 45 to 50 cm depth (hereafter called 10 and 50 cm) at 16 sites along two altitudinal transects spanning ~3,200 m of elevation, one across the eastern flank (~400 to ~3,400 m) and the other across the western flank (~200 to ~2,600 m) of the Eastern Cordillera of Colombia (Figure 2). At four sites on the western flank (218, 1,281, 2,185, and 2,589 m), we also collected an additional soil sample from a 25 to 30 cm depth to evaluate possible variations of brGDGTs with depth. In total, we collected 36 soil samples. Temperature data loggers (HOBO UA-001-08 8K) were installed at all 16 sites at the same two depths of 10 and 50 cm where we collected soil samples for analysis of brGDGTs, and we ensured that the loggers were fully inserted within the wall of the hole at the appropriate depths. We attached a string to each logger, and the holes were covered with the same material that was dug out, making sure that the end of the string was left exposed at the surface. Additionally, we installed air temperature loggers at each site ~2 m above the ground from the closest tree and at a distance <~15 m from the soil loggers. Soil and air temperature measurements were recorded every 2 hr from August 2017 to August 2018 (Table S1 in http://doi.org/10.5281/zenodo.3939270). We recovered all loggers, except for the two soil loggers from the lowest (~400 m) site on the eastern flank. Soil pH was measured in the field using an Oaktan waterproof pH 150 meter and a WD-35614-30 probe. We mixed ~2 g of soil with milli-Q water in a 1:2.5 (soil:water) ratio before each measurement and used a new container for each sample. We calibrated the pH meter at every third station using buffers with pH 4.00, 7.00, and 10.00.

3.2. brGDGT Analysis of Soil Samples

We freeze dried, homogenized, and sieved (0.3 mm) the soil samples to remove roots, plant debris, and coarse particles. In order to achieve maximum recovery of lipids from each sample, we extracted ~8 g of soil sample twice with dichloromethane:methanol (DCM:MeOH 9:1 v:v) using an accelerated solvent extractor (ASE 200 DIONEX; 100°C and 2,000 psi). We evaporated total lipid extracts (TLEs) under a gentle N_2 stream using a Turbovap and then combined and removed elemental sulfur using copper pellets previously activated with HCl for at least 1 hr. Later, we filtered the TLEs through a short Pasteur pipette filled with glass wool and sand:Na_2SO_4 (8:2) to remove any particles and water. Samples were spiked with 250 ng of the C_{46} GDGT internal standard (Huguet et al., 2006). Then, we dissolved the dry samples in 1 ml of hexane:isopropanol (hexane:IPA 99:1 v/v) and sonicated, vortexed, and filtered them through a 0.45-μm PTFE filter before injection.

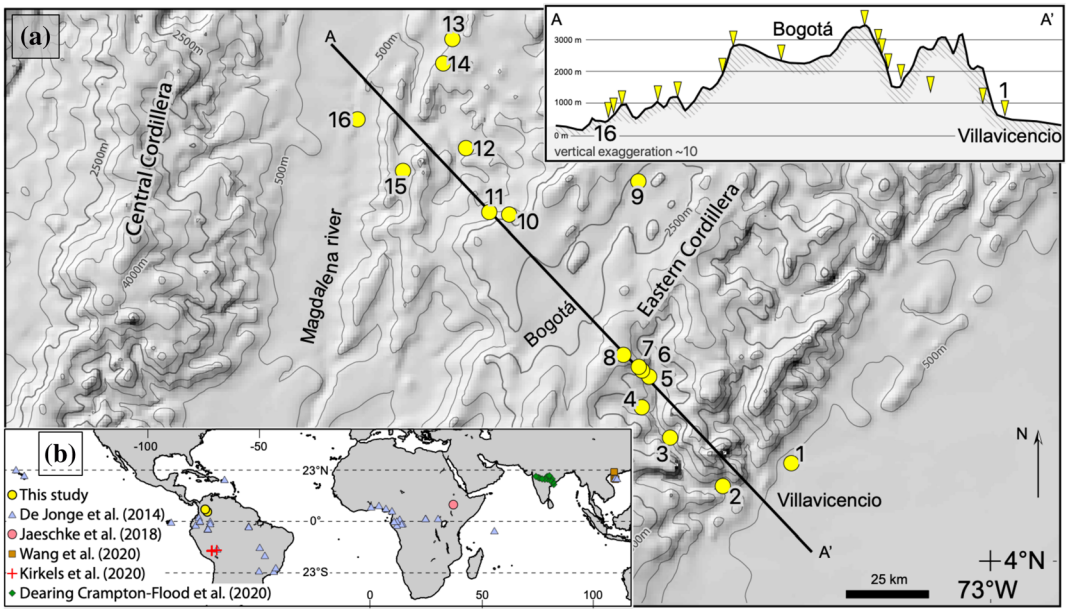

Figure 2. Study area. (a) Map of the Eastern Cordillera of Colombia for which the regional calibration was generated; yellow symbols indicate the 16 sites with new data presented in this study. The black line indicates the altitudinal transect (from A-A′) of the 16 soil sites shown in the insert in the upper right corner. (b) World map indicating the locations and corresponding references of soils around the tropics used in the tropical compilation.

We analyzed brGDGTs using a Thermo Scientific Ultimate 3000 high-performance liquid chromatograph (HPLC) coupled to a Q Exactive Focus Orbitrap-Quadrupole high-resolution mass spectrometer via an atmospheric pressure chemical ionization (APCI) source. We achieved the chromatographic separation, identification, and quantification of brGDGTs by using a slightly modified version of the protocol described by Hopmans et al. (2016). Rather than starting at 18% hexane:isopropanol (9:1, v/v) (Hopmans et al., 2016), we began the eluent gradient with 30% hexane:isopropanol (9:1, v/v) to shorten overall run times without compromising the chromotographic separation of brGDGTs (Crump et al., 2019; Harning et al., 2019; Figure S1 in the supporting information). We re-equilibrated the HPLC column for 20 min between runs. The injection volume was 10 μl instead of the 5 μl in Hopmans et al. (2016). The positive ion APCI settings are in Table S2 in the supporting information. We analyzed samples on full-scan mode with a mass range of 500–1,500 m/z at 70,000 mass resolution. We calibrated the Q Exactive within a mass accuracy range of 3 ppm using the Pierce LTQ Velos ESI Positive Ion Calibration Solution (Thermo Scientific). We identified the internal standard and brGDGTs based on their characteristic molecular ions (m/z 744, 1,050, 1,048, 1,046, 1,036, 1,034, 1,032, 1,022, 1,020, and 1,018) and elution patterns and performed manual integration of the area under each peak using the Thermo Scientific Xcalibur software. The analytical uncertainty, when estimating the area of each brGDGT measured in triplicate, is less than 0.08%.

3.3. Tropical Soil Data Set Compilation

We compiled existing brGDGTs data from sites within 23.5° of the equator from De Jonge et al. (2014), Dearing Crampton-Flood et al. (2020), Jaeschke et al. (2018), Kirkels et al. (2020), Naafs, Gallego-Sala, et al. (2017), and Wang et al. (2020) and combined them with the results from our study to create a brGDGT soil calibration that can be used for tropical paleoclimate reconstructions (Table S3 in http://doi.org/10.5281/zenodo.3939270). We included only sites for which 5- and 6-methyl isomers were separated, their FA was available, and their modern MAAT was published. We excluded four soils sites in the globally distributed compilation reported by De Jonge et al. (2014), also excluded by Naafs, Gallego-Sala, et al. (2017), because of their unknown elevation. De Jonge et al. (2014) and Naafs, Gallego-Sala, et al. (2017) inferred different values of MAAT, as large as 13°C for the same site. Naafs, Gallego-Sala, et al. (2017) interpolated temperatures from a gridded database with 0.5° of resolution in both latitude and longitude: When the elevation of a soil site fell inside a cell grid but differed by more than 250 m from the average elevation of that grid cell,

Naafs, Gallego-Sala, et al. (2017) used the temperature value of the nearest grid cell, whose elevation differed from that of site by less than 250 m. We consider that this approach is inappropriate for the tropics, where the biggest temperature differences derive from differences in elevation that can vary across short distances. Therefore, we decided to use the temperatures reported by De Jonge et al. (2014) for the tropical samples within this global soil compilation because they relied on air temperatures from the closest meteorological station. Jaeschke et al. (2018), Kirkels et al. (2020), and Wang et al. (2020) inferred their MAAT from nearby weather stations for their respective soil samples. Dearing Crampton-Flood et al. (2020) inferred values of MAAT associated to their new reported soil samples from the nearest gridded value extracted from the CRU TS v. 3.24.01 data set with a 0.5° resolution in both latitude and longitude. We noted the possible risks associated with this approach above, but given the lack of *in situ* measurements at these sites, we used the temperature reported by Dearing Crampton-Flood et al. (2020).

3.4. Statistical Analyses

We carried out simple linear regressions with the MBT'_{5me} index and multiple linear regressions to derive equations to estimate temperatures, first for the Eastern Cordillera of Colombia (hereafter Eastern Cordillera) and then for the tropics as a whole. We considered all 15 brGDGTs for the calculation of each FA. We regressed FAs of each brGDGTs against temperature, and those with statistically significant linear relationship with temperature, with p values < 0.01, were selected when calculating the multiple linear regressions. When performing all calculations, we represented each FA with four significant figures. We fitted various candidate relationships that relate brGDGTs to MAAT and mean annual soil temperature (MAST), each with different combinations of predictors. In each case, the predictors were FAs of individual brGDGT. For each candidate relationship or model, we computed the Bayesian Information Criterion (BIC, Equation 7; Schwarz, 1978) as follows:

$$\mathrm{BIC} = -2L + k^{*}\log(n), \tag{7}$$

where L is the log-likelihood function, k is the number of parameters estimated by the equation, and n is the number of observations. The first term corresponds to the mean squared error (i.e., goodness of fit), and the second term is a penalty for complexity of the equation (i.e., the number of parameters).

Compared to other such metrics, the BIC heavily favors parsimony, which enables reduced uncertainty in the model by way of fewer parameters. The candidate model with the least BIC was selected as the *multiple linear model* that best fitted the data. For the pantropical calibration, we considered candidate nonlinear models involving second- and third-degree terms of the potential predictor set of brGDGTs, the model with minimum BIC was selected as the *best nonlinear model*. If the uncertainty in a coefficient of a variable in the best model obtained by the BIC criterion exceeded the value of the coefficient, it was excluded from the final equation. To assess the relative variability and importance of the different brGDGTs, we performed principal component analysis (PCA). This offers diagnostic insights and is a complement to the regression models.

4. Results and Discussion

4.1. Soil and Air Temperatures From the Eastern Cordillera of Colombia

Mean monthly air temperatures (MMATs) and mean monthly soil temperatures (MMSTs) recorded by *in situ* loggers show a small temperature seasonality in this region, with the greatest difference between the mean warmest month and the mean coldest month for the same site of only 3.9°C for air, 3.7°C for soil at 10 cm, and 2.9°C for soil at 50 cm (Figure 3 and Table S1 in http://doi.org/10.5281/zenodo.3939270). Average temperature gradients with elevation across the entire Eastern Cordillera are 5.9 ± 0.2°C/km for air ~2 m above the ground, 5.2 ± 0.3°C/km for soil at a 10-cm depth, and 5.3 ± 0.3°C/km for soil at a 50-cm depth (Figure 4). The difference between soil (for both 10 and 50 cm) and air temperatures increases with elevation from approximately −0.5°C to ~2.5°C (indicating an elevation gradient of the difference of 0.7 ± 0.2°C/km; Figure 4). Since the MASTs measured at both 10 and 50 cm at each station of the Eastern Cordillera were almost identical, with an average absolute difference of 0.1°C (Figure 4), we included temperatures from both depths in the following calibrations.

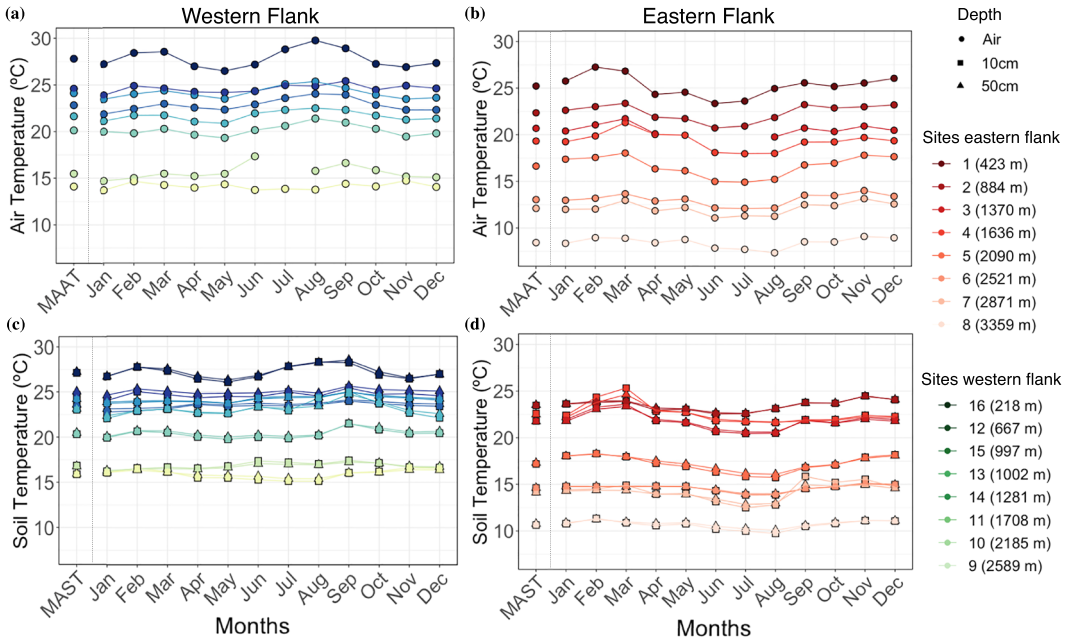

Figure 3. Mean *in situ* monthly temperatures recorded by data loggers from August 2017 to August 2018 along the two elevation transects in the Eastern Cordillera (Table S1 in http://doi.org/10.5281/zenodo.3939270). Panels (a) and (b) show the mean monthly air temperature (MMAT) for each flank. Panels (c) and (d) show the mean monthly soil temperature (MMST) at 10- and 50-cm depths for each flank.

4.2. Regional Soil brGDGTs Calibration for the Eastern Cordillera of Colombia

We compare the new measured soil brGDGTs data from the Eastern Cordillera with the measured pH and MAAT and MAST (Table S3 in http://doi.org/10.5281/zenodo.3939270) in Figures 5 and 6, respectively. We included all brGDGT except for IIIc′, as its FA comprises 0.005% of the data and it is present in only six of the 36 samples (Figure 6c). Most 6-methyl brGDGTs (II′ and III′ in Figure 5) show a higher correlation with pH than 5-methyl brGDGTs (II and III in Figure 5). 6-methyl brGDGT IIb′ shows the highest correlation with pH ($R^2 = 0.57$). Consistent with previous work (De Jonge et al., 2014), 6-methyl brGDGTs in the Eastern Cordillera do not show a significant correlation with MAAT or MAST (p values > 0.05, Figure 6a).

BrGDGT IIa correlates best with MAAT and MAST ($R^2 = 0.8$), followed by brGDGTs IIIa ($R^2 = 0.48$), Ib ($R^2 = 0.4$), and Ic ($R^2 = 0.4$) (Figure 6a). We performed the multiple linear calibration with only those brGDGTs that exhibit a p value < 0.01 when regressed against temperature. We used the modern soil brGDGTs data (Figure 6) and the MAAT and MAST derived from loggers (Figure 3) to develop air and soil temperature calibrations for the Eastern Cordillera. We use the MBT'_{5me} index to obtain a simple linear calibration in 8 and selected the multiple linear regression in 9 with the lowest BIC value:

$$\mathrm{MAST} = 1.65\ (\pm 1.85) + 23.58\ (\pm 2.31) \times \mathrm{MBT'_{5me}}\ \left(n = 30, R^2 = 0.79, \mathrm{RMSE} = 2.1°\mathrm{C}\right), \quad (8)$$

$$\mathrm{MAST} = 22.79\ (\pm 0.65) + 13.08\ (\pm 3.14) \times [\mathrm{Ib}] - 23.35\ (\pm 2.11) \times [\mathrm{IIa}] \quad (9)$$
$$\left(n = 30, R^2 = 0.90, \mathrm{RMSE} = 1.5°\mathrm{C}\right).$$

For the air temperature calibration, 10 uses the MBT'_{5me} index and the smallest BIC value using multiple linear regression yields 11:

$$\mathrm{MAAT} = -2.83\ (\pm 1.95) + 28.18\ (\pm 2.42) \times \mathrm{MBT'_{5me}}\ \left(n = 36, R^2 = 0.80, \mathrm{RMSE} = 2.4°\mathrm{C}\right), \quad (10)$$

$$\mathrm{MAAT} = 22.49\ (\pm 0.78) + 14.57\ (\pm 3.68) \times [\mathrm{Ib}] - 27.68\ (\pm 2.59) \times [\mathrm{IIa}] \quad (11)$$
$$\left(n = 36, R^2 = 0.87, \mathrm{RMSE} = 1.9°\mathrm{C}\right).$$

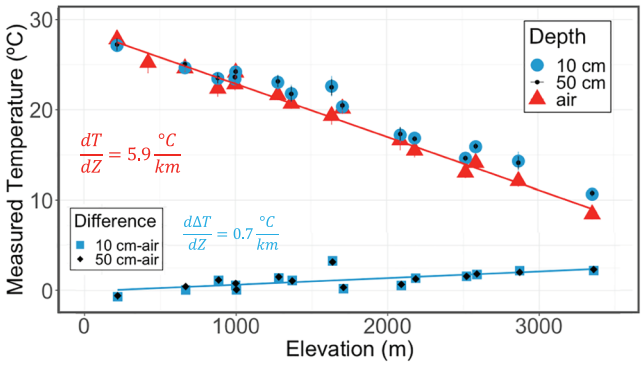

Figure 4. Mean *in situ* soil and air temperatures measured from August 2017 to August 2018 versus elevation. Top: data points show mean temperatures at 10 cm (blue circles) and 50 cm (black circles), and overlying air temperatures (red triangles), with their respective monthly standard deviations. The red line shows a gradient of air temperature relative to elevation (dT/dZ) in the Eastern Cordillera of 5.9 ± 0.2°C/km. Bottom: points show differences between mean temperatures of soil (at 10 cm as blue squares and at 50 cm as black diamonds) and air. The blue line shows a gradient of the difference in temperature relative to elevation ($d\Delta T/dZ$) of 0.7 ± 0.2°C/km.

Regressions 8 aned 10, using the MBT'_{5me} index, not only show a lower R^2 and higher RMSE than the multiple linear regressions 9 and 11, but also their temperature estimates saturate at 25.2°C for MAST and 25.3°C for MAAT. These saturations show that the MBT'_{5me} cannot reconstruct temperatures of the warmest sites in the Eastern Cordillera. Also, the uncertainty (±1.85) of the intercept in 8 is greater than its value (1.65), exemplifying its unreliability. Equations 9 and 11 incorporate the same brGDGTs, IIa and Ib, which are the second and third most abundant brGDGTs in the Eastern Cordillera (Figure 6c). Although brGDGTs Ic and IIIa correlate with temperature (Figure 6a), they also correlate well with Ib and IIa (Figure 6b), respectively. Therefore, in seeking a parsimonious set of predictors, the BIC criterion shows that only brGDGTs Ib and IIa are needed to estimate temperature values. The fit of Equation 9 for MAST is better than 11 for MAAT. This demonstrates that temperature estimates are more accurate when measuring the medium in which soil bacteria live, than the overlying air. In global calibrations (e.g., De Jonge et al., 2014; Weijers et al., 2007), brGDGT Ia plays a key role because of its association with warm environments, as also shown by its prominence in the Eastern Cordillera (Figure 6c). In that latter region, however, as in the tropics in general and shown below, it correlates insignificantly with temperature (p value > 0.05). Thus, even if Ia is the most abundant brGDGT in warm environments, it does not capture the temperature variability in these regions.

Both regional MAST and MAAT calibrations (9 and 11, respectively), reduce the RMSE substantially, from 4.6°C in 3 (De Jonge et al., 2014) and 3.8°C in 6 (Naafs, Gallego-Sala, et al., 2017), to 1.5°C for MAST and 1.9°C for MAAT (Figures 7a, 7b, 7d, and 7e). Moreover, all soil and air temperatures inferred by the regional calibrations differ from those measured with temperature loggers by less than 5°C (Figure 8). By contrast, global calibrations underestimate air temperatures for the Eastern Cordillera by up to 13.2°C. More than 70% of the soil samples from global calibrations were taken from mid-latitude areas where seasonal cycles reach 15–30°C. Global calibrations incorporate a wide range of environmental factors with a diverse

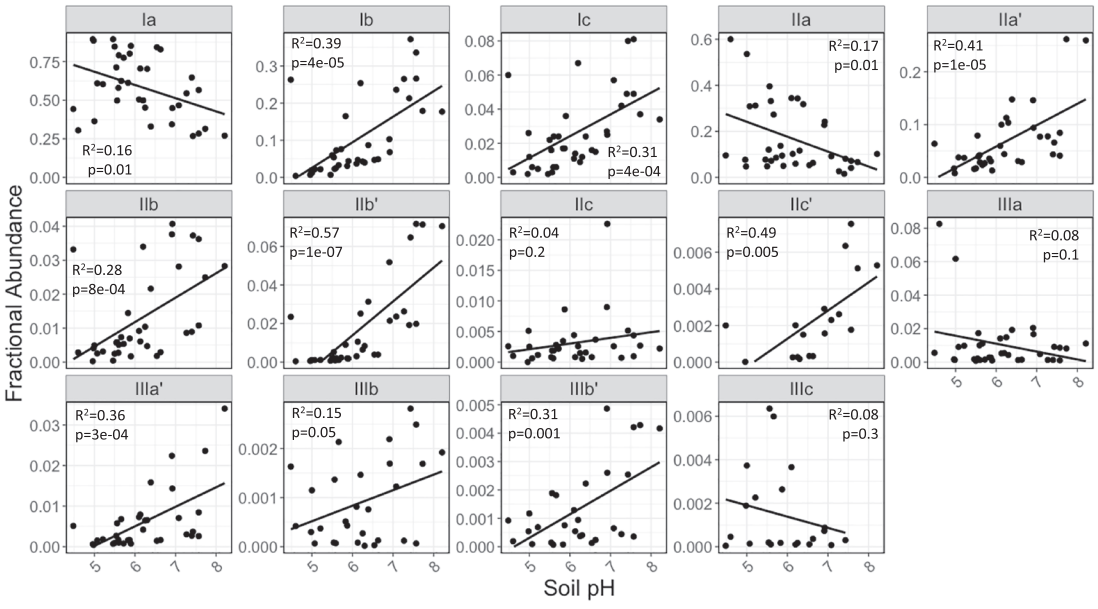

Figure 5. Regressions between fractional abundances of 14 brGDGTs and measured soil pH from the Eastern Cordillera with their corresponding values of p and R^2. We do not include brGDGTs present below the limit of quantification.

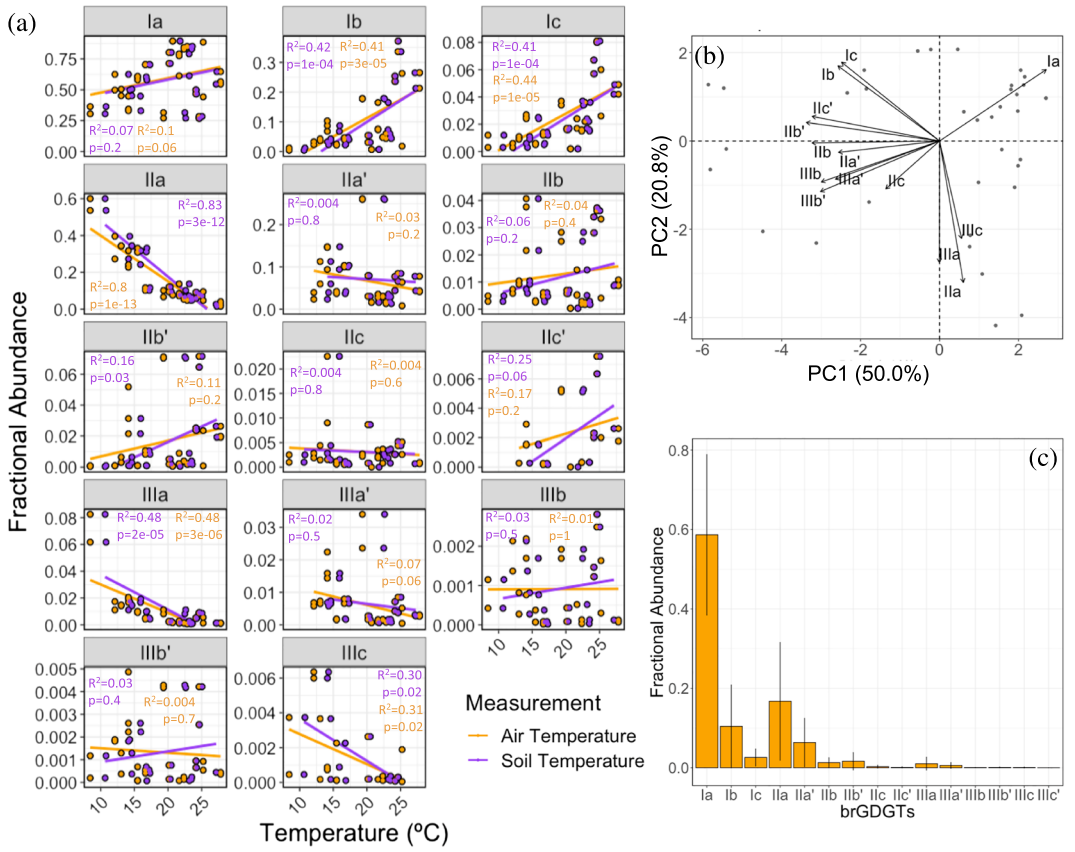

Figure 6. (a) Linear regressions between fractional abundances of 14 brGDGTs and measured mean annual air temperatures (orange) and mean annual soil temperatures (purple) of each soil in the Eastern Cordillera, including their corresponding values of p and R^2. We do not include brGDGTs present below the limit of quantification. (b) Principal components PC1 and PC2 of the main brGDGTs used in the temperature calibrations plotted against one another. (c) Average fractional abundances and standard deviation of each individual brGDGTs in the Eastern Cordillera.

bacterial community composition. The latter can contribute with lipid signatures that have no correlation with temperature (e.g., De Jonge et al., 2019). Therefore, regionally or latitudinally restricted calibrations could be more accurate when estimating past temperatures. These regional calibrations for the Eastern Cordillera not only allow for reconstruction of warmer temperatures than previous global calibrations do (De Jonge et al., 2014; Naafs, Gallego-Sala, et al., 2017; Peterse et al., 2012) but also include samples with higher measured temperatures, 27.8°C for air and 27.5°C for soil, than ~26°C in De Jonge et al. (2014). Extrapolations, however, of MAST and MAAT estimates outside these calibration ranges should be made with caution.

Previous work on the Eastern Cordillera by Anderson et al. (2014), which used soil temperature loggers but a chromatographic method that did not separate 5- and 6- methyl brGDGTs, yielded a local soil calibration with a RMSE of 2.9°C 12:

$$\begin{aligned}\mathrm{MAT} = {} & 29.1 - 0.017 \times (\mathrm{Ia}) - 0.61 \times \log(\mathrm{Ib}) - 3.34 \times \log(\mathrm{Ic}) - 0.34 \times (\mathrm{IIa}) - 0.11 \times \log(\mathrm{IIb}) \\ & + 0.44 \times \log(\mathrm{IIc}) - 0.067 \times (\mathrm{IIIa}) \left(n = 24, R^2 = 0.77, \mathrm{RMSE} = 2.9°\mathrm{C}\right), \end{aligned} \tag{12}$$

Although this equation resulted in an improvement over the RMSE of 5°C from the global air temperature calibration (Peterse et al., 2012), this RMSE value (2.9°C) is still higher than what can be obtained when 6-methyl brGDGTs are chromatographically separated and excluded 9 (Figure 9). The influence of 6-methyl brGDGTs is particularly noticeable at the warm sites (>15°C), where the calibration from Anderson et al. (2014) underestimates temperatures by as much as ~9°C. Furthermore, for sites

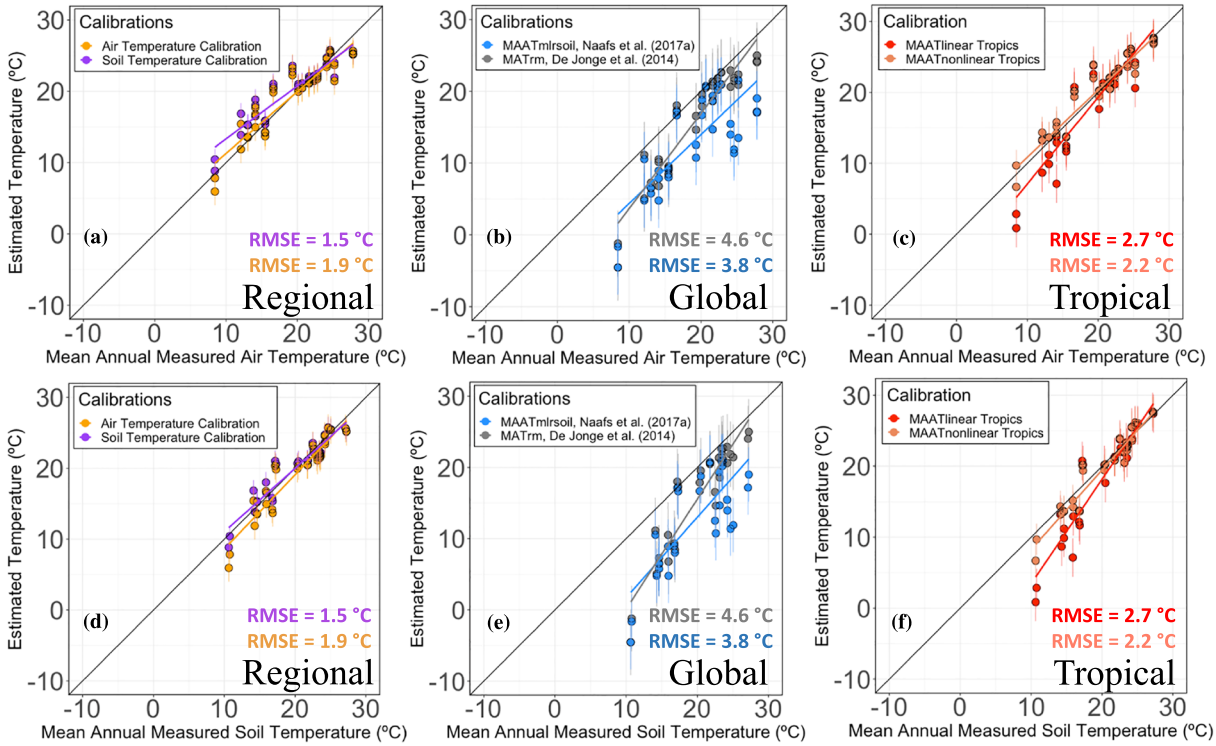

Figure 7. Regressions of estimated temperatures against measured (a, b, and c) mean annual air temperatures and (d, e, and f) mean annual soil temperatures from August 2017 to August 2018 in the Eastern Cordillera, using temperatures estimated with different brGDGT calibrations. (a and d) Temperatures inferred from brGDGTs are compared using the regional calibrations for air temperatures (orange) 11 and soil temperatures (purple) 9. (b and e) Temperature values are compared with global calibrations 3 and 6 from De Jonge et al. (2014) (gray) and Naafs, Gallego-Sala, et al. (2017) (light blue). (c and f): Temperature values are compared with the pantropical calibrations 14 and 15. Black lines represent 1:1 relationships.

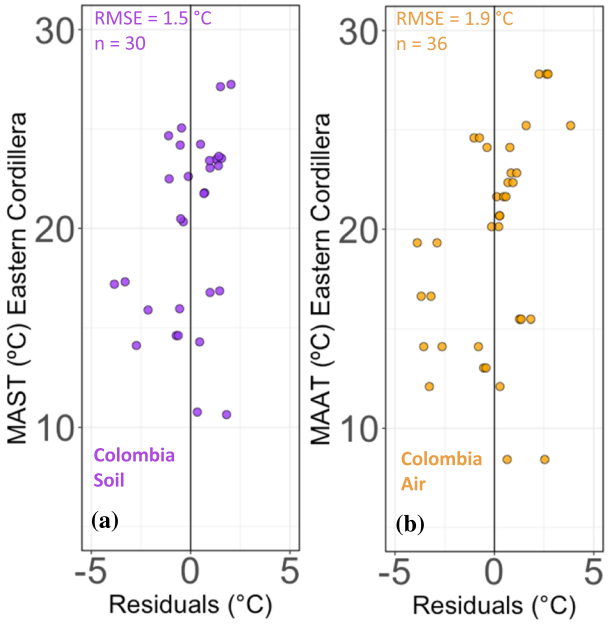

Figure 8. Residuals for the multiple linear regressions calculated in (a) the soil temperature (MAST) calibration of the Eastern Cordillera and (b) the air temperature (MAAT) calibration of the Eastern Cordillera.

where we measured MAST, we obtained an $R^2 = 0.90$ for the soil calibration in 9 compared to the $R^2 = 0.52$ for the soil calibration of Anderson et al. (2014). This improvement confirms the utility of separating 5- and 6-methyl brGDGTs when estimating temperatures.

4.3. A Pantropical brGDGT Soil Calibration

In order to incorporate the new data obtained from the Eastern Cordillera into data sets from elsewhere in the tropics, we compared the FA of each individual brGDGT with the available measured pH (Figure 10) and MAAT (Figure 11) for each soil ($n = 175$) in the tropical compilation (Table S3 in http://doi.org/10.5281/zenodo.3939270). As shown by De Jonge et al. (2014) and our data from the Eastern Cordillera (Figure 5), the 6-pentamethyl brGDGTs (II′ in Figure 10) exhibit a higher correlation with pH than the 5-pentamethyl (II in Figure 10) in the soil samples from the tropical compilation. The highest correlation with pH comes from brGDGT Ib ($R^2 = 0.66$) followed by IIb′ ($R^2 = 0.62$) and IIa′ ($R^2 = 0.60$).

BrGDGT IIa correlates best with MAAT ($R^2 = 0.67$; Figure 11a), and brGDGTs IIIa, IIc′, Ib, and IIb′ also correlate well with temperature in tropical areas where the seasonal cycle of temperature is small. Opposite to the Eastern Cordillera and global data (De Jonge et al., 2014), brGDGTs IIa′, IIb′, IIc′, and IIIa′ have $p$values < 0.01 when regressed against MAAT (Figure 11a). We chose to

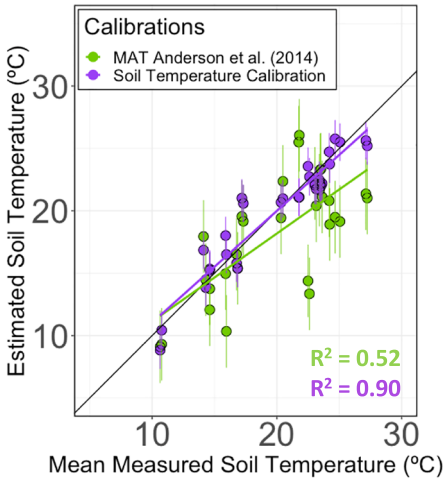

Figure 9. Comparison between the soil calibration 12 from Anderson et al. (2014) (green line) and the regional soil calibration 9 (purple line) with soil temperature measurements from the Eastern Cordillera. Black line represents 1:1 relationship.

incorporate all brGDGTs with p values < 0.01 in regressions with temperature when calculating the multiple linear regression that fits the tropical data the best. The FAs of some brGDGTs (i.e., Ib, IIa′, and IIIa′) show a nonlinear distributions for the highest temperatures in the tropics (Figure 11a). To allow nonlinear dependences, we also fit polynomial regressions of second degree and third degree to all the brGDGTs and compared their significance with linear fits using BIC. We included only terms in the nonlinear multiple regression that exhibit p values < 0.01 when regressed with temperature (Table S4 in http://doi.org/10.5281/zenodo.3939270). When all tropical data are used, the MBT'_{5me} index results in 13 and according to the BIC criterion, the best fits for linear and nonlinear multiple regressions are 14 and 15:

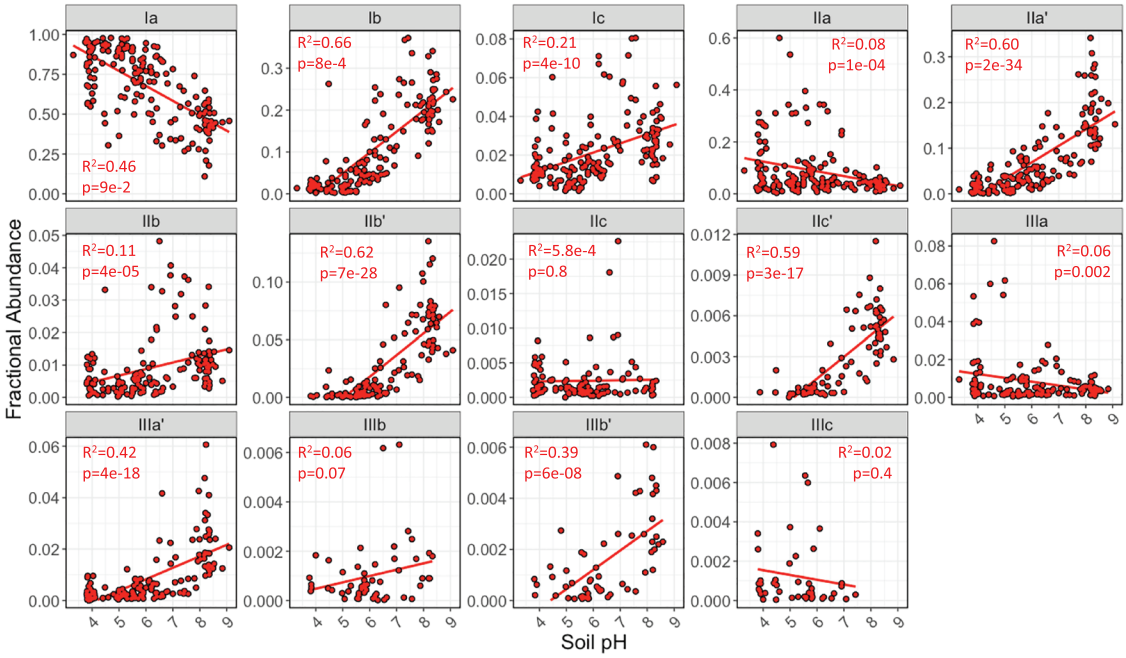

Figure 10. Linear regressions between fractional abundances (FAs) of brGDGTs and measured soil pH from the compilation of brGDGT measurements from the tropics, with the corresponding values of p and R^2. Only three out of 175 soil samples do not have pH measurements. We do not include brGDGTs present below the limit of quantification.

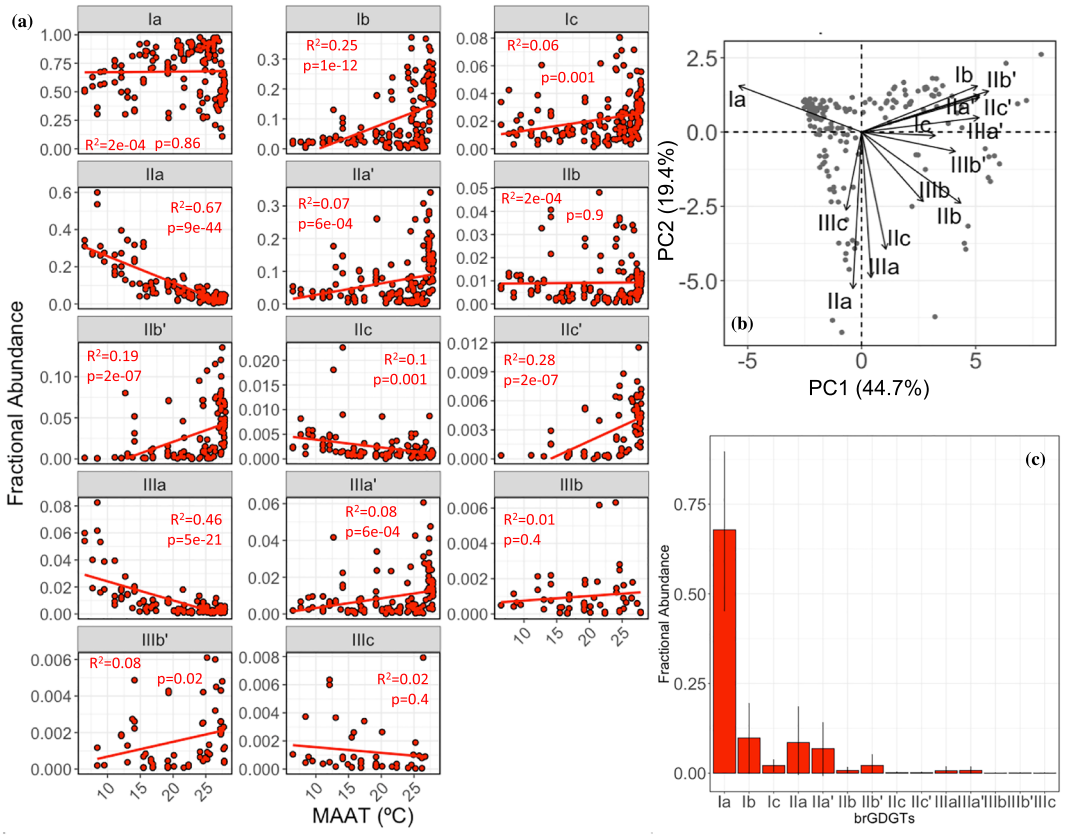

Figure 11. (a) Linear regressions between fractional abundances of 14 brGDGTs and measured mean annual air temperatures (MAATs) of each soil in the tropical compilation, with the corresponding values of p and R^2. We do not include brGDGTs present below the limit of quantification. (b) Principal components PC1 and PC2 of the 14 brGDGTs plotted against each other. (c) Average fractional abundances and standard deviation of each individual brGDGTs in the tropical calibration ($n = 175$).

$$\mathrm{MAAT}_{\mathrm{TropicsMBT}} = -11.76\ (\pm 2.01) + 38.13\ (\pm 2.25) \times \mathrm{MBT'}_{\mathrm{5me}}\ \left(n = 175, R^2 = 0.62, \mathrm{RMSE} = 3.5°\mathrm{C}\right), \quad (13)$$

$$\mathrm{MAAT}_{\mathrm{linearTropics}} = 24.12\ (\pm 0.39) + 18.28\ (\pm 2.25) \times [\mathrm{Ib}] - 38.23\ (\pm 2.36) \times [\mathrm{IIa}] - 397.23\ (\pm 83.04) \times [\mathrm{IIc}]\ \left(n = 175, R^2 = 0.78, \mathrm{RMSE} = 2.7°\mathrm{C}\right), \quad (14)$$

$$\mathrm{MAAT}_{\mathrm{nonlinearTropics}} = 25.29\ (\pm 0.34) + 15.55\ (\pm 1.85) \times [\mathrm{Ib}] - 66.58\ (\pm 2.83) \times [\mathrm{IIa}] + 92.94\ (\pm 10.38) \times [\mathrm{IIa}]^2 - 1788.65\ (\pm 562.31) \times [\mathrm{IIIa}]^2\ \left(n = 175, R^2 = 0.85, \mathrm{RMSE} = 2.2°\mathrm{C}\right). \quad (15)$$

The simple linear regression, using the $\mathrm{MBT'}_{\mathrm{5me}}$ index 13, yields a lower R^2 and a higher RMSE than 14 and 15, as we found in the Eastern Cordillera when comparing the $\mathrm{MBT'}_{\mathrm{5me}}$ index equation with the multiple linear regressions using FAs. Moreover, 13 saturates at 26.4°C, which prevents the $\mathrm{MBT'}_{\mathrm{5me}}$ index from reconstructing temperatures of soils where the MAAT can be as warm as 27.9°C. Multiple linear regression 14 shows an improvement in R^2 (0.78) and RMSE (2.7°C) compared to 13 ($R^2 = 0.62$ and RMSE = 3.5°C). Also, 14 relies on the same brGDGTs as both MAST and MAAT calibrations for the Eastern Cordillera 9 and 11, as well as IIc, suggesting that variations in temperature in the tropics are best captured by brGDGTs Ib and IIa in linear regressions. Although the RMSE (2.7°C) for the MAAT in the tropics is

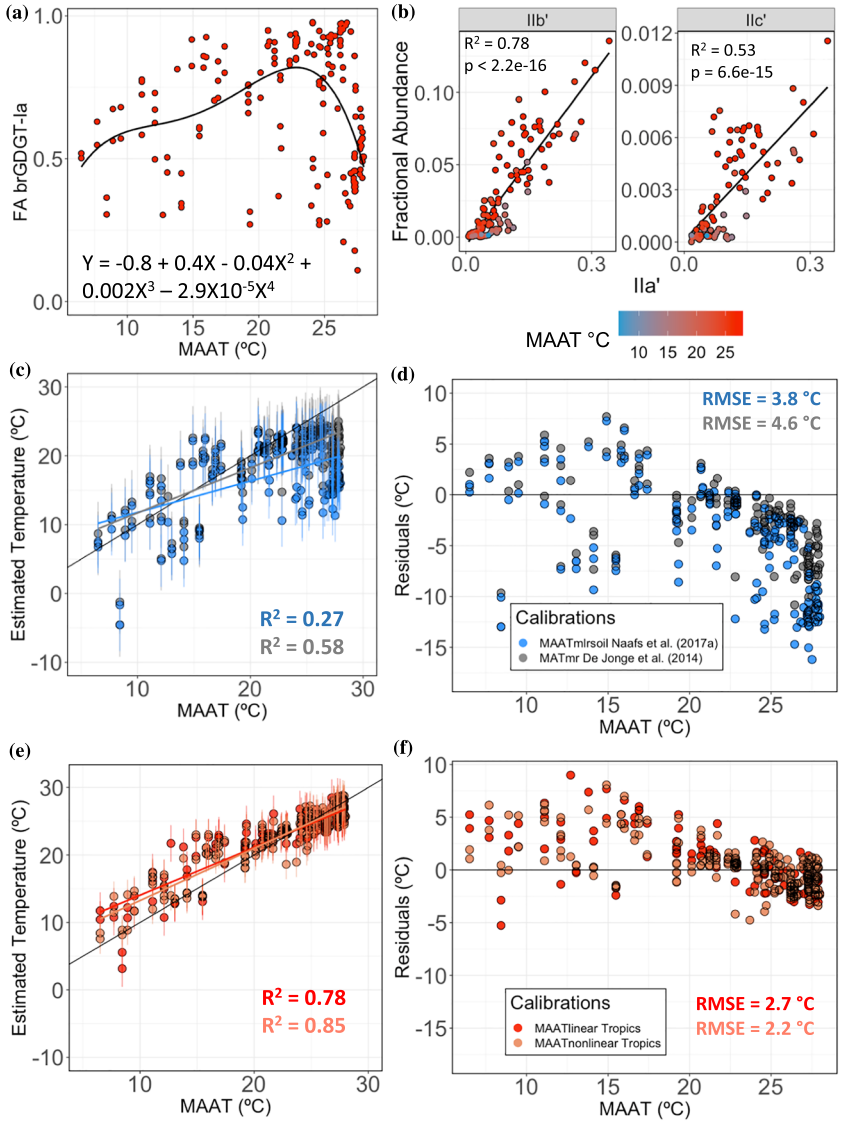

Figure 12. (a) Fractional abundance of brGDGT Ia against mean annual air temperatures (MAATs) in the tropics with a polynomial fit of fourth degree. (b) Linear regressions between brGDGTs IIb′ and IIc′ against IIa′, with the corresponding values of p and R^2. We do not include brGDGTs present below the limit of quantification. (c) Temperature estimates using global 3 and 6 calibrations for all tropical sites. (d) Residuals of the temperature estimates in panel (b). (e) Temperature estimates using the two tropical calibrations from this study 14 and 15 for all tropical sites. (f) Residuals of the temperature estimates in panel (d).

greater than that for the Eastern Cordillera (1.9°C in 11), it is more than 1°C smaller than those of global calibrations (RMSE = 3.8–4.6°C; Figure 7). This improvement highlights the importance of latitudinally restricted calibrations, which embody a more limited range of environments over the global calibrations. Thus, latitudinally restricted calibration could likely include a less heterogeneous bacterial community composition. Equation 15, which involves nonlinear predictors, incorporates an additional brGDGT (IIIa) into the calibration, and includes terms with quadratic dependence. This equation shows a slight improvement in the R^2 (0.85) and RMSE (2.2°C) compared to 14 when estimating temperature values. More importantly, 15 highlights the importance of nonlinear parameters when considering the warmest temperatures in soils around the globe. We suggest the use of Equation 14 or 15 in paleoreconstructions, though extrapolations to higher temperatures should be made with caution.

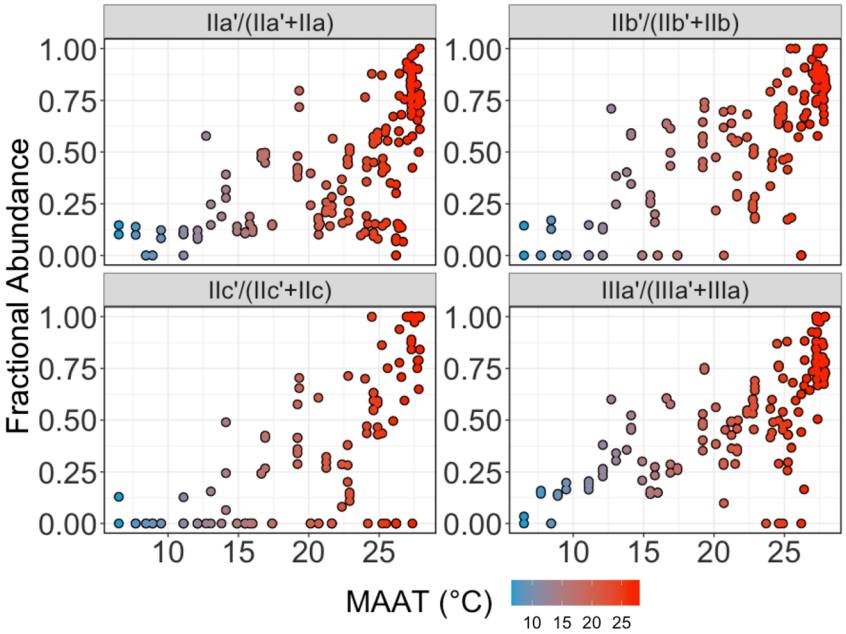

Figure 13. Fractional abundance ratios of 6-methyl brGDGTs with respect to the sum of corresponding 5- and 6-methyl isomers against mean annual air temperature (MAAT) in the tropical compilation (n = 175).

In general, the FA for brGDGT Ia is, by far, the highest in warm and tropical regions, with an average of 68% overall (Figure 11c). Its abundance, however, does not correlate linearly with temperature (Figure 11a). In the tropics, the FA of brGDGT Ia becomes a multivalued function of temperature (Figure 12a). In global calibrations with MAAT from appriximately −5°C to ~25°C, the linear relationship of the FA of brGDGT Ia to temperature makes it one of the most important predictors when estimating MAAT (see Fig. 8 in De Jonge et al., 2014 and Fig. 2 in Naafs, Gallego-Sala, et al., 2017). The FA of brGDGT Ia correlates negatively, however, with temperature in areas warmer than ~22°C in the tropics (Figure 12a). This result suggests that using brGDGT Ia cannot, yet at least, be used to estimate temperature in the tropics or warm environments.

Existing global calibrations underestimate temperature in tropical sites by as much as ~ −16°C (Figures 12c and 12d). When considering sites with lower temperatures, which in the tropics are high elevation sites, the tropical calibrations slightly overestimate temperatures, where the calibration is least well resolved (Figures 12e and 12f). The nonlinear calibration 15 is more accurate than the linear calibration 14 when estimating the colder temperatures, suggesting that 15 should be used when deducing paleoelevations from

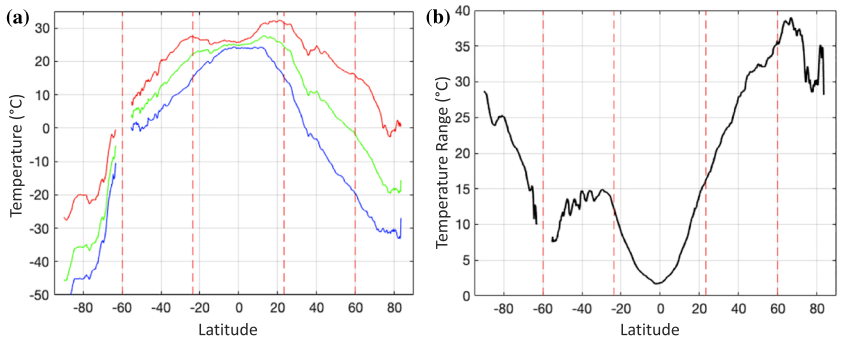

Figure 14. (a) Zonally averaged mean air temperatures at 2 m above land areas (obtained from climate Copernicus ERA5 data). Mean annual air temperature (green), mean warmest month (red), and mean coldest month (blue). (b) Zonally averaged mean annual range of air temperature calculated as the difference between the warmest month and the coldest month for each site. Dashed red lines mark the limits of the tropical region in addition to the 60th parallel.

temperatures in tropical areas. A possible explanation for this overestimation is the limited number of sites (27 out of 175) with a MAAT below 15°C in the tropical compilation, which may lead to biases toward warmer conditions. Another possible contribution to this overestimation could be the observed increasing difference between soil and air temperatures with increasing elevation (Figure 4), where bacteria living in high-elevation soils (>3,000 m) register the warmer temperature of the soil compared to the colder overlying air (Figure 7).

The FAs of 6-pentamethyl brGDGTs increase at temperatures warmer than ~19°C, and they correlate with each other as temperature increases (Figure 12b). Indeed, the 6-methyl brGDGTs increase with respect to their 5-methyl isomer with increasing temperature, particularly toward the warmer range of the tropics (Figure 13). When considering nonlinear approaches to estimate temperature and restricted to the warm end of the tropical compilation, brGDGTs IIa′ and IIb′ become part of the equation that best estimates temperature values (Figure 13). Russell et al. (2018) also reported that some 6-methyl brGDGTs correlate with temperature in East African lakes. FAs of brGDGTs Ib, IIa, IIa′, and IIb′ increase or decrease with temperature similarly in East African lakes as tropical soils.

Global calibrations of MAAT rely on soil bacteria that live at different latitudes and that can grow at different times within a year, but the specific timing of growth for brGDGT-producing bacteria remains unknown. Therefore, temperature estimates that are calibrated with global MAAT could misrepresent the temperatures that bacteria record. If bacterial growth were biased toward warmer rather than colder days, global calibrations would underestimate temperature. In order to quantify the typical temperature variability in an annual cycle at different latitudes, we obtained terrestrial air temperature data from around the world for the 2000–2018 period from the European Centre for Medium Range Weather Forecasts (ECMWF) Reanalysis version 5 (ERA5) with a resolution of 0.25° in both latitude and longitude (Hersbach et al., 2019; Figure 14). The mean annual range of temperature by latitude, calculated as the difference between the warmest month and the coldest month for terrestrial temperatures, shows that the tropics have the smallest difference compared to the rest of the globe (Figure 14b). The tropics are the only place where all of the regressions of brGDGT abundances against MAAT, mean annual temperature above freezing, and warmest months are similar enough that they can all represent the same value. Thus, whether brGDGT-based temperature calibrations might be better constrained by regional calibrations limited to restricted latitudinal ranges outside the tropics rather than global generalizations remains to be seen.

5. Conclusions

The combination of (1) *in situ* temperatures measured in soils at depths of 10 and 50 cm and in the air 2 m above the ground along profiles spanning 3,200 m on the eastern and western sides of the Eastern Cordillera of Colombia and (2) measured fractional abundances of the different brGDGTs in them yields temperature calibrations that differ markedly from those derived from mid- and high-latitude environments. Simple linear regressions (8, 10, and 13) show that the MBT'_{5me} index is not appropriate for estimating temperature in tropical soils as they saturate at 24–26°C. We obtained linear equations 9 and 11 that relate the fractional abundances of brGDGTs Ib and IIa to soil and overlying air temperatures with RMSE of 1.5°C and 1.9°C, respectively. Combining these data with published measurements from other sites in the tropics (<23.5° latitude), we obtained a linear calibration of air temperature 14 with a RMSE of 2.7°C and a nonlinear calibration 15 with a RMSE of 2.2°C, which we recommend for use in paleostudies throughout the tropics. This pantropical compilation demonstrates the importance of some 6-methyl brGDGTs when considering temperatures above ~19°C. These calibrations contrast with, and improve upon, global calibrations with RSME of 3.8–4.9°C. Tropical calibrations are not subject to possible seasonal biases, as mean monthly temperatures differ little from the mean annual values. Moreover, these calibrations avoid the use of brGDGT Ia, whose fractional abundance follows a multivalued function of temperature. Finally, they extend the temperature range accessible by brGDGTs to temperatures typical of low latitudes, which is necessary for brGDGTs to be used to infer past temperatures from tropical environments, especially during intervals warmer than at present, such as the Early Pliocene, Eocene, and Cretaceous.

Data Availability Statement

The soil data set is archived in Zenodo data repository and is freely and publicly available online, and may be accessed directly as http://doi.org/10.5281/zenodo.3939270. Global climate data used in this study are freely and publicly available online, and may be accessed directly as ECMWF Reanalysis version 5: https://cds.climate.copernicus.eu/#!/search?text=ERA5&type=dataset.

Acknowledgments

This research was supported by the Fondo Corrigan-ACGGP-ARES (Colombia), a Lewis and Clark grant, CIRE's Innovative Research Program (IRP) 2017, a CIRES Graduate Student Research Award, a Figueroa Family Grant from the Graduate School at University of Colorado Boulder, an Edward Fellowship from the Department of Geological Sciences at the University of Colorado Boulder, the DIDI (Dirección de Investigación, Desarrollo e Innovación) from Universidad del Norte, the Facultad de Ciencias from Universidad de Los Andes, and NSF Sedimentary Geology and Paleobiology grant 1929199. J.S. acknowledges laboratory and analytical support provided by the University of Colorado Boulder. L.P.A. thanks K. Karnauskas for his help with the ERA5 data acquisition and MATLAB coding, and J. Yarce for his help with MATLAB. We thank K. Quinn, N. Kentwortz, K. Amara, and J. Smith for laboratory support, C.A. Rosero, R. Villamil, M.E. Angel-Olaya, E. Pérez-Angel, and F. Gutierrez for assistance in the field, and local residents in Colombia who helped us and allowed us to install temperature loggers on their properties. We thank A. Jaeschke, E. Dearing Crampton-Flood, and F. Kirkels for providing additional information from their manuscripts to the tropical compilation set and H. Wang for a preprint of his paper in advance of publication. The data used in this study are listed under Data Availability Statement and cited in the references. We thank two anonymous reviewers for their constructive and helpful suggestions, two times each, that improved the manuscript.

References

Anderson, V. J., Saylor, J. E., Shanahan, T. M., & Horton, B. K. (2015). Paleoelevation records from lipid biomarkers: Application to the tropical Andes. *Bulletin*, *127*(11–12), 1604–1616. https://doi.org/10.1130/B31105.1

Anderson, V. J., Shanahan, T. M., Saylor, J. E., Horton, B. K., & Mora, A. R. (2014). Sources of local and regional variability in the MBT′/CBT paleotemperature proxy: Insights from a modern elevation transect across the Eastern Cordillera of Colombia. *Organic Geochemistry*, *69*, 42–51. https://doi.org/10.1016/j.orggeochem.2014.01.022

Crump, S. E., Miller, G. H., Power, M., Sepúlveda, J., Dildar, N., Coghlan, M., & Bunce, M. (2019). Arctic shrub colonization lagged peak postglacial warmth: Molecular evidence in lake sediment from Arctic Canada. *Global Change Biology*, *25*(12), 4244–4256. https://doi.org/10.1111/gcb.14836

Dang, X., Yang, H., Naafs, B. D. A., Pancost, R. D., & Xie, S. (2016). Evidence of moisture control on the methylation of branched glycerol dialkyl glycerol tetraethers in semi-arid and arid soils. *Geochimica et Cosmochimica Acta*, *189*, 24–36. https://doi.org/10.1016/j.gca.2016.06.004

De Jonge, C., Hopmans, E. C., Zell, C. I., Kim, J. H., Schouten, S., & Sinninghe Damsté, J. S. (2014). Occurrence and abundance of 6-methyl branched glycerol dialkyl glycerol tetraethers in soils: Implications for palaeoclimate reconstruction. *Geochimica et Cosmochimica Acta*, *141*, 97–112. https://doi.org/10.1016/j.gca.2014.06.013

De Jonge, C., Radujković, D., Sigurdsson, B. D., Weedon, J. T., Janssens, I., & Peterse, F. (2019). Lipid biomarker temperature proxy responds to abrupt shift in the bacterial community composition in geothermally heated soils. *Organic Geochemistry*, *137*, 103897. https://doi.org/10.1016/j.orggeochem.2019.07.006

Dearing Crampton-Flood, E., Tierney, J. E., Peterse, F., Kirkels, F. M., & Sinninghe Damsté, J. S. (2020). BayMBT: A Bayesian calibration model for branched glycerol dialkyl glycerol tetraethers in soils and peats. *Geochimica et Cosmochimica Acta*, *268*, 142–159. https://doi.org/10.1016/j.gca.2019.09.043

Dearing Crampton-Flood, Emily; Tierney, Jessica E; Peterse, Francien; Kirkels, Frédérique M S A; Sinninghe, Damsté, Jaap, S (2019). Global soil and peat branched GDGT compilation dataset. PANGAEA, https://doi.org/10.1594/PANGAEA.907818, Supplement to: Dearing Crampton-Flood, E et al. (2020): BayMBT: A Bayesian calibration model for branched glycerol dialkyl glycerol tetraethers in soils and peats. Geochimica et Cosmochimica Acta, *268*, 142–159, https://doi.org/10.1016/j.gca.2019.09.043

Dekens, P. S., Ravelo, A. C., & McCarthy, M. D. (2007). Warm upwelling regions in the Pliocene warm period. *Paleoceanography*, *22*, PA3211. https://doi.org/10.1029/2006PA001394

Delgado-Baquerizo, M., Oliverio, A. M., Brewer, T. E., Benavent-González, A., Eldridge, D. J., Bardgett, R. D., et al. (2018). A global atlas of the dominant bacteria found in soil. *Science*, *359*(6373), 320–325. https://doi.org/10.1126/science.aap9516

Deng, L., Jia, G., Jin, C., & Li, S. (2016). Warm season bias of branched GDGT temperature estimates causes underestimation of altitudinal lapse rate. *Organic Geochemistry*, *96*, 11–17. https://doi.org/10.1016/j.orggeochem.2016.03.004

Ding, S., Xu, Y., Wang, Y., He, Y., Hou, J., Chen, L., & He, J. S. (2015). Distribution of branched glycerol dialkyl glycerol tetraethers in surface soils of the Qinghai-Tibetan Plateau: Implications of brGDGTs-based proxies in cold and dry regions. *Biogeosciences*, *12*(11), 3141–3151. https://doi.org/10.5194/bg-12-3141-2015

Ghosh, P., Adkins, J., Affek, H., Balta, B., Guo, W., Schauble, E. A., et al. (2006). 13C–18O bonds in carbonate minerals: A new kind of paleothermometer. *Geochimica et Cosmochimica Acta*, *70*(6), 1439–1456. https://doi.org/10.1016/j.gca.2005.11.014

Groeneveld, J., Steph, S., Tiedemann, R., Garbe-Schönberg, C., Nürnberg, D., & Sturm, A. (2006). *Pliocene mixed-layer oceanography for site 1241, using combined Mg/Ca and $\delta^{18}O$ analyses of Globigerinoides sacculifer* (Vol. 202, pp. 1–27). Paper presented at Proceedings of the Ocean Drilling Program: Scientific Results. https://doi.org/10.2973/odp.proc.sr.202.209.2006

Halpert, M. S., & Ropelewski, C. F. (1992). Surface temperature patterns associated with the Southern Oscillation. *Journal of Climate*, *5*, 577–593. https://doi.org/10.1175/1520-0442(1992)005<0577:STPAWT>2.0.CO;2

Hanna, A. J., Shanahan, T. M., & Allison, M. A. (2016). Distribution of branched GDGTs in surface sediments from the Colville River, Alaska: Implications for the MBT′/CBT paleothermometer in Arctic marine sediments. *Journal of Geophysical Research: Biogeosciences*, *121*, 1762–1780. https://doi.org/10.1002/2015JG003266

Harning, D. J., Andrews, J. T., Belt, S. T., Cabedo-Sanz, P., Geirsdóttir, Á., Dildar, N., et al. (2019). Sea ice control on winter subsurface temperatures of the North Iceland Shelf during the Little Ice Age: A TEX_{86} calibration case study. *Paleoceanography and Paleoclimatology*.

Herbert, T. D., Lawrence, K. T., Tzanova, A., Peterson, L. C., Caballero-Gill, R., & Kelly, C. S. (2016). Late Miocene global cooling and the rise of modern ecosystems. *Nature Geoscience*, *9*(11), 843–847. https://doi.org/10.1038/ngeo2813

Herbert, T. D., Peterson, L. C., Lawrence, K. T., & Liu, Z. (2010). Tropical ocean temperatures over the 3.5 million years. *Science*, *328*(5985), 1530–1534. https://doi.org/10.1126/science.1185435

Hersbach, H., Bell, W., Berrisford, P., Horányi, A., Sabater, J. M., Nicolas, J., et al. (2019). Global reanalysis: Goodbye ERA-Interim, hello ERA5. *ECMWF newsletter*, *159*, 17–24. https://doi.org/10.21957/vf291hehd7

Hooghiemstra, H., Wijninga, V. M., & Cleef, A. M. (2006). The paleobotanical record of Colombia: Implications for biogeography and biodiversity. *Annals of the Missouri Botanical Garden*, *93*(2), 297–325. https://doi.org/10.3417/0026-6493(2006)93%5B297:TPROCI%5D2.0.CO;2

Hopmans, E. C., Schouten, S., & Sinninghe Damsté, J. S. (2016). The effect of improved chromatography on GDGT-based palaeoproxies. *Organic Geochemistry*, *93*, 1–6. https://doi.org/10.1016/j.orggeochem.2015.12.006

Huguet, C., Hopmans, E. C., Febo-Ayala, W., Thompson, D. H., Sinninghe Damsté, J. S., & Schouten, S. (2006). An improved method to determine the absolute abundance of glycerol dibiphytanyl glycerol tetraether lipids. *Organic Geochemistry*, *37*(9), 1036–1041. https://doi.org/10.1016/j.orggeochem.2006.05.008

Jaeschke, A., Rethemeyer, J., Lappé, M., Schouten, S., Boeckx, P., & Schefuß, E. (2018). Influence of land use on distribution of soil n-alkane δD and brGDGTs along an altitudinal transect in Ethiopia: Implications for (paleo)environmental studies. *Organic Geochemistry*, *124*, 77–87. https://doi.org/10.1016/j.orggeochem.2018.06.006

Kirkels, F. M., Ponton, C., Galy, V., West, A. J., Feakins, S. J., & Peterse, F. (2020). From Andes to Amazon: Assessing branched tetraether lipids as tracers for soil organic carbon in the Madre de Dios River system. *Journal of Geophysical Research: Biogeosciences*, *125*(1). https://doi.org/10.1029/2019JG005270

Kirkels, Frédérique M S A; Ponton, Camilo; Galy, Valier; West, A Joshua; Feakins, Sarah J; Peterse, Francien (2019). Analysis of brGDGTs as tracers for soil organic carbon in the Madre de Dios River system. PANGAEA, https://doi.org/10.1594/PANGAEA.906170, supplement to: Kirkels, FMSA et al. (2019): From Andes to Amazon: assessing branched tetraether lipids as tracers for soil Organic Carbon in the Madre de Dios River system. Journal of Geophysical Research: Biogeosciences, https://doi.org/10.1029/2019JG005270

Lawrence, K. T., Liu, Z., & Herbert, T. D. (2006). Evolution of the eastern tropical Pacific through Plio-Pleistocene glaciation. *Science*, *312*(5770), 79–83. https://doi.org/10.1126/science.1120395

Liang, J., Russell, J. M., Xie, H., Lupien, R. L., Si, G., Wang, J., et al. (2019). Vegetation effects on temperature calibrations of branched glycerol dialkyl glycerol tetraether (brGDGTs) in soils. *Organic Geochemistry*, *127*, 1–11. https://doi.org/10.1016/j.orggeochem.2018.10.010

Liu, X.-L., Leider, A., Gillespie, A., Gröger, J., Versteegh, G. J. M., & Hinrichs, K.-U. (2010). Identification of polar lipid precursors of the ubiquitous branched GDGT orphan lipids in a peat bog in northern Germany. *Organic Geochemistry*, *41*(7), 653–660. https://doi.org/10.1016/j.orggeochem.2010.04.004

Liu, X.-L., Summons, R. E., & Hinrichs, K.-U. (2012). Extending the known range of glycerol ether lipids in the environment: Structural assignments based on tandem mass spectral fragmentation patterns. *Rapid Communications in Mass Spectrometry*, *26*(19), 2295–2302. https://doi.org/10.1002/rcm.6355

Liu, X.-L., Zhu, C., Wakeham, S. G., & Hinrichs, K.-U. (2014). In situ production of branched glycerol dialkyl glycerol tetraethers in anoxic marine water columns. *Marine Chemistry*, *166*, 1–8. https://doi.org/10.1016/j.marchem.2014.08.008

Loomis, S. E., Russell, J. M., & Lamb, H. F. (2015). Northeast African temperature variability since the Late Pleistocene. *Palaeogeography, Palaeoclimatology, Palaeoecology*, *423*, 80–90. https://doi.org/10.1016/j.palaeo.2015.02.005

Lu, H., Liu, W., Wang, H., & Wang, Z. (2016). Variation in 6-methyl branched glycerol dialkyl glycerol tetraethers in Lantian loess–paleosol sequence and effect on paleotemperature reconstruction. *Organic Geochemistry*, *100*, 10–17. https://doi.org/10.1016/j.orggeochem.2016.07.006

Menges, J., Huguet, C., Alcañiz, J. M., Fietz, S., Sachse, D., & Rosell-Melé, A. (2014). Influence of water availability in the distributions of branched glycerol dialkyl glycerol tetraether in soils of the Iberian Peninsula. *Biogeosciences*, *11*(10), 2571–2581. https://doi.org/10.5194/bg-11-2571-2014

Naafs, B. D. A., Gallego-Sala, A. V., Inglis, G. N., & Pancost, R. D. (2017). Refining the global branched glycerol dialkyl glycerol tetraether (brGDGT) soil temperature calibration. *Organic Geochemistry*, *106*, 48–56. https://doi.org/10.1016/j.orggeochem.2017.01.009

Naafs, B. D. A., Inglis, G. N., Zheng, Y., Amesbury, M. J., Biester, H., Bindler, R., et al. (2017). Introducing global peat-specific temperature and pH calibrations based on brGDGT bacterial lipids. *Geochimica et Cosmochimica Acta*, *208*, 285–301. https://doi.org/10.1016/j.gca.2017.01.038

Peterse, F., Martínez-García, A., Zhou, B., Beets, C. J., Prins, M. A., Zheng, H., & Eglinton, T. I. (2014). Molecular records of continental air temperature and monsoon precipitation variability in East Asia spanning the past 130,000 years. *Quaternary Science Reviews*, *83*, 76–82. https://doi.org/10.1016/j.quascirev.2013.11.001

Peterse, F., van der Meer, J., Schouten, S., Weijers, J. W. H., Fierer, N., Jackson, R. B., et al. (2012). Revised calibration of the MBT–CBT paleotemperature proxy based on branched tetraether membrane lipids in surface soils. *Geochimica et Cosmochimica Acta*, *96*, 215–229. https://doi.org/10.1016/j.gca.2012.08.011

Ravelo, A. C., Dekens, P. S., & McCarthy, M. (2006). Evidence for El Niño-like conditions during the Pliocene. *GSA Today*, *16*(3), 4. https://doi.org/10.1130/1052-5173(2006)016<4:EFENLC>2.0.CO;2

Ropelewski, C. F., & Halpert, M. S. (1987). Global and regional scale precipitation patterns associated with the El Niño/Southern Oscillation. *Monthly Weather Review*, *115*(8), 1606–1626. https://doi.org/10.1175/1520-0493(1987)115<1606:GARSPP>2.0.CO;2

Ropelewski, C. F., & Halpert, M. S. (1989). Precipitation patterns associated with the high index phase of the Southern Oscillation. *Journal of Climate*, *2*(3), 268–284. https://doi.org/10.1175/1520-0442(1989)002<0268:PPAWTH>2.0.CO;2

Russell, J. M., Hopmans, E. C., Loomis, S. E., Liang, J., & Sinninghe Damsté, J. S. (2018). Distributions of 5- and 6-methyl branched glycerol dialkyl glycerol tetraethers (brGDGTs) in East African lake sediment: Effects of temperature, pH, and new lacustrine paleotemperature calibrations. *Organic Geochemistry*, *117*, 56–69. https://doi.org/10.1016/j.orggeochem.2017.12.003

Salzmann, U., Dolan, A. M., Haywood, A. M., Chan, W.-L., Voss, J., Hill, D. J., et al. (2013). Challenges in quantifying Pliocene terrestrial warming revealed by data-model discord. *Nature Climate Change*, *3*(11), 969–974. https://doi.org/10.1038/nclimate2008

Sarachik, E. S., & Cane, M. A. (2010). *The El Niño-Southern Oscillation phenomenon* (p. 369). Cambridge, UK: Cambridge University Press. https://doi.org/10.1017/CBO9780511817496

Schwarz, G. (1978). Estimating the dimension of a model. *The Annals of Statistics*, *6*(2), 461–464. https://doi.org/10.1214/aos/1176344136

Sinninghe Damsté, J. S., Hopmans, E. C., Pancost, R. D., Schouten, S., & Geenevasen, J. A. J. (2000). Newly discovered non-isoprenoid glycerol dialkyl glycerol tetraether lipids in sediments. *Journal of the Chemical Society, Chemical Communications*, *2000*, 1683–1684.

Sinninghe Damsté, J. S., Rijpstra, W. I. C., Foesel, B. U., Huber, K. J., Overmann, J., Nakagawa, S., et al. (2018). An overview of the occurrence of ether-and ester-linked iso-diabolic acid membrane lipids in microbial cultures of the Acidobacteria: Implications for brGDGT paleoproxies for temperature and pH. *Organic Geochemistry*, *124*, 63–76. https://doi.org/10.1016/j.orggeochem.2018.07.006

Sinninghe Damsté, J. S., Rijpstra, W. I. C., Hopmans, E. C., Weijers, J. W. H., Foesel, B. U., Overmann, J., & Dedysh, S. N. (2011). 13,16-Dimethyl octacosanedioic acid (iso-diabolic acid), a common membrane-spanning lipid of acidobacteria subdivisions 1 and 3. *Applied and Environmental Microbiology*, *77*(12), 4147–4154. https://doi.org/10.1128/aem.00466-11

Thomas, E. K., Clemens, S. C., Sun, Y., Huang, Y., Prell, W., Chen, G., et al. (2017). Midlatitude land surface temperature impacts the timing and structure of glacial maxima. *Geophysical Research Letters*, *44*, 984–992. https://doi.org/10.1002/2016GL071882

Torres, V., Vandenberghe, J., & Hooghiemstra, H. (2005). An environmental reconstruction of the sediment infill of the Bogotá Basin (Colombia) during the last 3 million years from abiotic and biotic proxies. *Palaeogeography, Palaeoclimatology, Palaeoecology*, *226*(1–2), 127–148. https://doi.org/10.1016/j.palaeo.2005.05.005

Trenberth, K. E., Branstator, G. W., Karoly, D., Kumar, A., Lau, N. C., & Ropelewski, C. (1998). Progress during TOGA in understanding and modeling global teleconnections associated with tropical sea surface temperatures. *Journal of Geophysical Research*, *103*(C7), 14,291–14,324. https://doi.org/10.1029/97JC01444

van der Hammen, T., Werner, J. H., & van Dommelen, H. (1973). Palynological record of the upheaval of the northern Andes: A study of the Pliocene and Lower Quaternary of the Colombian Eastern Cordillera and the early evolution of its High-Andean biota. *Review of Paleobotany and Palynology*, *16*(1-2), 1–122. https://doi.org/10.1016/0034-6667(73)90031-6

Wang, H., An, Z., Lu, H., Zhao, Z., & Liu, W. (2020). Calibrating bacterial tetraether distributions towards in situ soil temperature and application to a loess-paleosol sequence. *Quaternary Science Reviews*, *231*, 106172. https://doi.org/10.1016/j.quascirev.2020.106172

Wang, H., Liu, W., & Lu, H. (2016). Appraisal of branched glycerol dialkyl glycerol tetraether-based indices for North China. *Organic Geochemistry*, *98*, 118–130. https://doi.org/10.1016/j.orggeochem.2016.05.013

Wang, H., Liu, W., & Zhang, C. L. (2014). Dependence of the cyclization of branched tetraethers on soil moisture in alkaline soils from arid-subhumid China: Implications for palaeorainfall reconstructions on the Chinese Loess Plateau. *Biogeosciences*, *11*(23), 6755–6768. https://doi.org/10.5194/bg-11-6755-2014

Wara, M. W., Ravelo, A. C., & Delaney, M. L. (2005). Permanent El Niño-like conditions during the Pliocene warm period. *Science*, *309*(5735), 758–761. https://doi.org/10.1126/science.1112596

Weber, Y., de Jonge, C., Rijpstra, W. I. C., Hopmans, E. C., Stadnitskaia, A., Schubert, C. J., et al. (2015). Identification and carbon isotope composition of a novel branched GDGT isomer in lake sediments: Evidence for lacustrine branched GDGT production. *Geochimica et Cosmochimica Acta*, *154*, 118–129. https://doi.org/10.1016/j.gca.2015.01.032

Weber, Y., Sinninghe Damsté, J. S., Zopfi, J., de Jonge, C., Gilli, A., Schubert, C. J., et al. (2018). Redox-dependent niche differentiation provides evidence for multiple bacterial sources of glycerol tetraether lipids in lakes. *Proceedings of the National Academy of Sciences*, *115*(43), 10,926–10,931. https://doi.org/10.1073/pnas.1805186115

Weijers, J. W. H., Panoto, E., Van Bleijswijk, J., Schouten, S., Rijpstra, I. C., Balk, M., et al. (2009). Constraints on the biological source (s) of the orphan branched tetraether membrane lipids. *Geomicrobiology Journal*, *26*(6), 402–414. https://doi.org/10.1080/01490450902937293

Weijers, J. W. H., Schouten, S., Hopmans, E. C., Geenevasen, J. A. J., David, O. R. P., Coleman, J. M., et al. (2006). Membrane lipids of mesophilic anaerobic bacteria thriving in peats have typical archaeal traits. *Environmental Microbiology*, *8*(4), 648–657. https://doi.org/10.1111/j.1462-2920.2005.00941.x

Weijers, J. W. H., Schouten, S., van den Donker, J. C., Hopmans, E. C., & Sinninghe Damsté, J. S. (2007). Environmental controls on bacterial tetraether membrane lipid distribution in soils. *Geochimica et Cosmochimica Acta*, *71*(3), 703–713. https://doi.org/10.1016/j.gca.2006.10.003

Wolfe, J. A. (1995). Paleoclimatic estimates from Tertiary leaf assemblages. *Annual Review of Earth and Planetary Sciences*, *23*(1), 119–142. https://doi.org/10.1146/annurev.ea.23.050195.001003

Yamamoto, Y., Ajioka, T., & Yamamoto, M. (2016). Climate reconstruction based on GDGT-based proxies in a paleosol sequence in Japan: Postdepositional effect on the estimation of air temperature. *Quaternary International*, *397*, 380–391. https://doi.org/10.1016/j.quaint.2014.12.009

Yang, H., Lü, X., Ding, W., Lei, Y., Dang, X., & Xie, S. (2015). The 6-methyl branched tetraethers significantly affect the performance of the methylation index (MBT′) in soils from an altitudinal transect at Mount Shennongjia. *Organic Geochemistry*, *82*, 42–53. https://doi.org/10.1016/j.orggeochem.2015.02.003

Yang, H., Pancost, R. D., Dang, X., Zhou, X., Evershed, R. P., Xiao, G., et al. (2014). Correlations between microbial tetraether lipids and environmental variables in Chinese soils: Optimizing the paleo-reconstructions in semi-arid and arid regions. *Geochimica et Cosmochimica Acta*, *126*, 49–69. https://doi.org/10.1016/j.gca.2013.10.041

Zachos, J. C., Pagani, M., Sloan, L., Thomas, E., & Billups, K. (2001). Trends, rhythms, and aberrations in global climate 65 Ma to present. *Science*, *292*(5517), 686–693. https://doi.org/10.1126/science.1059412